Nationaal Lucht- en Ruimtevaartlaboratorium

National Aerospace Laboratory NLR

NLR-TP-97511

The description of crack growth on the basis of the strip-yield model for computation of crack opening loads, the crack tip stretch and strain rates

A.U. de Koning, H.J. ten Hoeve and T.K. Hendriksen

NLR TECHNICAL REPORT

TP 97511 L

THE DESCRIPTION OF CRACK GROWTH ON THE BASIS

OF THE STRIP-YIELD MODEL FOR COMPUTATION

OF CRACK OPENING LOADS, THE CRACK TIP

STRETCH AND STRAIN RATES

by

A.U. de Koning, H.J. ten Hoeve and

T.K. Henriksen[*]

[*]   European Space Agency (ESA), ESTEC Noordwijk.

Division	: Structures and Materials	Completed	: 971010
Prepared	: AUdK/ HJtH/	Order number	: 542.302
Approved	: HHO/	Typ.	: JS

Contents

(23 pages in total)

Second Symposium on Advances in Fatigue Crack Closure

Measurement and Analysis

A.U. de Koning[1], H.J. ten Hoeve[1] and T.K. Henriksen[2]

The description of crack growth on the basis of the strip-yield model for computation of crack opening loads, the crack tip stretch and strain rates

[1] National Aerospace Laboratory (NLR), NOP, Netherlands
[2] European Space Agency (ESA), ESTEC, Noordwijk, Netherlands

Abstract: Nowadays, the application of the STRIP-YIELD model for computation of crack opening load levels is well known. In this paper the incremental formulation of a fatigue crack growth law is used to demonstrate the role of the crack opening load level in time independent fatigue crack growth.
Less known is the ability of the STRIP-YIELD model to define the strain rate at the crack tip. A threshold level $\dot{\varepsilon}_{th}$ of this strain rate is introduced and used to formulate a criterion for initiation of time dependent accelerated fatigue crack growth. This process is called corrosion fatigue. To account for effects of environment and frequency on the crack growth rate a time dependent part is added to the incremental fatigue crack growth law. The resulting incremental crack growth equation is integrated to obtain the crack growth rate for a load cycle.

The model discussed in this paper is a mechanical model. Physical aspects other than the strain rate, the loading frequency and load wave shape are not modelled in an explicit way. Hence, the model is valid for specific environment/base metal combinations. However, in a consideration of the effects of small variations of environment, temperature and other variables on the crack growth rates, it can be used as a reference solution.

The fatigue crack growth model has been implemented in the NASGRO (ESACRACK) software. The time dependent part is still subject of further evaluation.

Introduction
For over two decades models of fatigue crack growth have been based on empirical laws that relate the amount of crack growth in a load cycle to the stress intensity factor range $\Delta K = K_{max} - K_{min}$ or the effective [1] range $\Delta K_{eff} = K_{max} - K_{op}$. Correction factors were included for near threshold behaviour and accelerated growth in the high K regime.
From a physical point of view such crack growth laws are speculative because crack growth and plastic deformation are

irreversible processes that depend on the loading history. By
nature, such processes must be described in an incremental way
and properly integrated to obtain the amount of crack growth
for a load cycle or the part of a load cycle for which the
incremental description is valid [2,3]. Clearly, such a new
description allows that a distinction is made between the part
of a load range where secondary (cyclic) plastic flow is
observed and the part where primary plastic flow developes
under monotonic increasing loads. For each of these domains an
incremental crack growth law can be formulated. Then after
integration over the appropriate load ranges the contributions
to the crack growth rate for the load cycle under
consideration, are obtained. In a similar way "range pair" (or
"rain flow") principles may be used to select the appropriate
load ranges [4]. In addition, the incremental formulation
allows the introduction of other terms representing time and/or
environment dependent crack growth [5].

In this paper the STRIP-YIELD model is applied for
computation of crack opening loads, crack tip stretches and
strain rates. In the open literature [6,7] and other documents
[8,9] the STRIP-YIELD model is discussed extensively and,
recently, results obtained using different versions of the
model (the NASA/FASTRAN and the ESA/NLR versions) were compared
and it was concluded that the models predict the same crack
opening behaviour if the constraint effects on yielding are
modelled in the same way. For this reason the STRIP-YIELD model
itself is not discussed in detail. Instead, the description of
the STRIP-YIELD model is limited to the yield limits and the
equations used in this paper.

The definition of crack size c, crack tip stretch δ as
well as the assumptions made to account for differences in the
yield limit in tension $\overline{\sigma}_t$ compared to the yield limit in
compression $\overline{\sigma}_c$ are shown in figure 1. The introduction of a
separate parameter $\overline{\sigma}_c$ allows for some form of description of
different constraint, crack tip geometry and the effect of cold
work on yielding in compression. The material in the thin
Dugdale strip is assumed to behave in a rigid, ideal plastic
manner and elastic deformations are assumed to be absent in the
strip.

The assumed yield limits $\overline{\sigma}_t$ and $\overline{\sigma}_c$ can be introduced in
the STRIP-YIELD model. The result can be used to derive some
simple analytical expressions for the crack tip stretch δ. For
monotonic increasing loads it can be derived, as a first order
approximation and for small scale yielding, that

$$\delta = K^2 / E\overline{\sigma}_t \qquad\qquad\qquad (1)$$

where K denotes the stress intensity factor and E is Youngs'
modulus. For the loading parts of a constant amplitude load

sequence we can derive in a similar way

$$\delta = K_{max}^2 / E\overline{\sigma}_t \underbrace{} - \left(K_{max} - K_{op}\right)^2 / E\left(\overline{\sigma}_t + \overline{\sigma}_c\right) \underbrace{} + \left(K - K_{op}\right)^2 / E\left(\overline{\sigma}_t + \overline{\sigma}_c\right) \underbrace{}$$

loading   unloading   loading

   to K_{max} from $K_{max} \rightarrow K_{op}$ from $K_{op} \rightarrow K$ (2)

$$K_{op} \leq K \leq K_{max}$$

where K_{op} is the stress intensity factor at the crack opening
load level. It is seen that for $K = K_{max}$ this equation gives
the same stretch as equation 1. Below K_{op} the plastic stretch
increment associated with unloading is assumed to be absent.
Also the effect of crack closure during unloading in the regime
$K_{max} \rightarrow K_{op}$ is ignored.
Equation 2 will be used to derive a simple expression for the
strain rate. More accurate results can be obtained by
application of the numerical discretized STRIP-YIELD model.
Which of both methods is used for computation of the crack tip
stretch depends on the efficiency and accuracy required in the
predicted results.

<u>Crack opening and threshold effects under fatigue loading
conditions</u>
      Usually, fatigue crack growth is assumed to occur in the
upward part of a load cycle. In the upward part different
regimes can be distinguished, depending on the loading history
and the state of opening of the crack. To illustrate these
domains in figure 2 the loading path is shown in a stress
intensity factor, K, versus crack size, c, plot. The different
loading regimes are indicated and discussed one after another
[5].

Closed crack regime 1, $K_{min} \leq K < K_{op}$
      Starting at the minimum intensity factor K_{min} the load is
increased until the crack opening level K_{op} is attained. In
this regime 1, characterized by $K_{min} \leq K < K_{op}$, the crack is at
least partly closed and the contact areas on the crack surfaces
decrease when the applied load is increased. Although the
stress intensity factors in this regime are calculated assuming
the presence of the crack, it is clear that the effective
loading of the crack tip region is very small and no crack
growth is assumed in this regime.

Opened crack but no growth regime 2, $K_{op} \leq K < K_{op} + \delta K_{th}$
      At level K_{op} the crack is fully opened, but, it takes
another increase by δK_{th} to initiate crack growth. Obviously,

some crack tip blunting occurs in this regime. Models and empirical equations for computation of values for K_{op} and δK_{th} are discussed in reference 5.

Fatigue crack growth in regime 3, $K_{op} + \delta K_{th} \leq K < K_*$

Upon a further increase of the applied load crack growth is initiated when the stress intensity factor K exceeds the level $K_{op} + \delta K_{th}$. In this regime 3 plastic deformations take place in a relatively small part of the plastic zone created by application of K_{max} in the previous load cycle. At the load level $K = K_*$ primary plastic flow in virgin material reinitiates and the zone of material that actually is loaded to the yield limit is extending beyond the previous plastic zone. The level K_* depends on the amount of crack growth relative to the primary plastic zone size. This transition is characterized by a discrete jump in plastic zone size and a loss of load history effects on the state of deformation. To describe the crack growth behaviour in regime 3, corresponding to $K_{op} + \delta K_{th} < K \leq K_*$, the following incremental crack growth law is adopted

$$dc_f = \left[C_1 \left(K - K_{op} \right)^{n_1} + C_2 \, \delta K_{th}^{\, p_1} \left(K - K_{op} \right)^{n_1 - p_1} \right] dK \tag{3}$$

where subscript f stands for fatigue.
In this expression the first term on the right hand side is an incremental form of Elbers' law. The second one is added to describe threshold effects, if present. The power $n_1 - p_1$ follows from the requirement that the units of both terms must be the same. Note that C_1, and n_1, are not the same as the traditional Elber parameters C and n ($C_1 = nC$; $n_1 = n-1$).
At initiation of crack growth, when, $K = K_{op} + \delta K_{th}$, it follows that

$$\left(\frac{dc_f}{dK} \right)_{th} = \delta K_{th}^{\, n_1} \left(C_1 + C_2 \right) \tag{4}$$

It may be expected that a relation exists between the material parameters C_1 and C_2, the threshold level δK_{th} and the slope of the crack growth curve (see Fig. 2).
In equation 3 the transition from threshold behaviour to the crack growth behaviour in the mid range (Elber) regime is governed by the power p_1 attached to $K-K_{op}$. Values selected for p_1 must guarantee that the transition is smooth and that the slope arctan(dc_f/dK) has the proper value. In order to simplify the equations in this application we use p_1 values satisfying

the equation

$$\left(\frac{dc_f}{dK} \right)_{th} = p_1 \, C_1 \, \delta K_{th}^{\, n_1} / \left(n_1 + 1 \right) \tag{5}$$

In that case, it follows from equation 4, that

$$C_2 = C_1 \frac{p_1 - n_1 - 1}{n_1 + 1} \tag{6}$$

To obtain the contribution of regime 3 to the crack growth rate per load cycle $\Delta c_f / \Delta N$ the crack growth law, equation 3, must be integrated over the range $K_{op} + \delta K_{th} \leq K \leq K_*$. It is assumed that the parameters involved (K_*, K_{op}, δK_{th}) are constant during integration. Then, after substitution of equation 6 and redefinition of the material and threshold parameters, there results

$$\Delta c_f / \Delta N = C \left(K_* - K_{op} \right)^n \left[1 - \left(\frac{\delta K_{th}}{K_* - K_{op}} \right)^{p_1} \right] \tag{7}$$

where K_* is the level at which the transition from cyclic, secondary, plastic flow to primary plastic flow occurs. In the absence of primary plastic flow ($K_* > K_{max}$) K_* is substituted by K_{max} and then equation 7 is the crack growth rate for the load cycle under consideration.

Note that also after integration the $\Delta c_f / \Delta N$ versus $K_{max} - K_{op}$ curve tends to be linear near threshold when K_* and K_{max} both tend towards $K_{op} + \delta K_{th}$. The slope can be determined from

$$d \left(\Delta c_f / \Delta N \right) / dK = p_1 C \, \delta K_{th}^{n-1} \tag{8}$$

Recently, Döker [11] confirmed experimentally that the relation between $\Delta c_f / \Delta N$ and $\Delta K = K_{max} - K_{min}$ is linear in the low ΔK regime when plotted on a linear scale. The present model fully supports Dökers ideas for a modification of the ASTM standard for threshold determination. After establishment of values for δK_{th}, C and n equation 8 can be used to derive a value for p_1 from the slope of the crack growth curve in the near threshold domain.

Quasi-static crack extension regime 4, $K_* \leq K \leq K_{max}$
    Loading above the transition level K_* is assumed to induce quasi-static crack extension. In this regime the plastic deformation behaviour takes place under monotonic increasing loads. This implies that the effects of secondary cyclic loading on the actual material behaviour are lost. Thus, the crack opening load and threshold behaviour becomes insignificant [2,3]. Moreover, the plastic zone sizes are much larger. To describe crack growth in this domain we will adopt the incremental formulation of the R (or J) curve approach. Assuming small scale plastic behaviour and small amounts of static crack extension the crack growth law adopted is written

NLR

as

$$dc_p = C_p K^m dK \qquad (9)$$

where subscript p denotes primary plastic flow in virgin
material.
In addition, for cases where wide scale plastic deformation
occurs or the amount of static crack extension becomes large we
may choose to introduce new -or sub- regimes and formulate the
applicable crack growth law in such a way that it describes
these processes properly.
The incremental crack growth law must be integrated over the
applicable range to obtain the contribution Δc_p to the crack
growth increment for a load cycle. There results

$$\Delta c_p / \Delta N = \frac{C_p}{m+1} \left[K_{max}^{m+1} - K_*^{m+1} \right] \qquad (10)$$

Regime 4 is discussed here for the sake of completeness. In
references 2, 3 and 5 the effect of quasi static growth of a
fatigue crack is discussed in detail. In the same references
equations for computation of δK_{th}, K_* and K_{op} are given.

Time dependent loading and definition of the stretch and strain
rate at the crack tip
        In an early publication of Speidel [10] on corrosion
fatigue some experimental observations were attributed to the
crack opening behaviour. An example is given in figure 3
reproduced from reference 10. The process is corrosion fatigue
and for one cycle from a constant amplitude sequence the crack
size is plotted versus time. The load ratio R equals 0. Hence,
based on crack opening functions from the open literature, it
is expected that the crack is open at a K level of
approximately 27 MPa√m. In any case far below the level of
about 47 MPa√m where accelerated growth initiates (see Fig. 3).
This difference is not covered by δK_{th} in regime 2. The
frequency effects in figure 4 and results shown by Barsom (Fig.
5) clearly demonstrate a rate effect. It is suggested here that
the stain rate at the crack tip appears to control the crack
growth process. In this section equations for computation of
the crack tip stretch and strain rate are discussed. In the
next section a crack growth law for the description of
corrosion fatigue is presented.

        Since crack growth can be ignored for stress intensity
levels below the opening level K_{op}, it is convenient to write
the prescribed time dependent stress intensity factor in the
following way

$$K(t) = K_{op} + \left(K_{max} - K_{op} \right) f(t) \qquad (11)$$

Some load shape functions are given in appendix A. After

substitution of equation 11 into equation 2 the crack tip
stretch can be written as

$$\delta(t) = \frac{K_{max}^2}{E\overline{\sigma}_t} + \frac{\left(K_{max} - K_{op}\right)^2}{E\left(\overline{\sigma}_t + \overline{\sigma}_c\right)}\left(f^2(t) - 1\right) \tag{12}$$

and for the stretch rate $d\delta(t)/dt$ it follows

$$d\delta(t)/dt = 2\frac{\left(K_{max} - K_{op}\right)^2}{E\left(\overline{\sigma}_t + \overline{\sigma}_c\right)} f(t) \quad df(t)/dt \tag{13}$$

Then, for the stain rate $\dot{\varepsilon}(t)$, according to the definition of
natural strain it follows that

$$\dot{\varepsilon}(t) = d\delta(t)/\delta(t)dt = \frac{2(1-CF)^2 f(t) df(t)/dt}{\beta + (1-CF)^2(f^2(t)-1)} \tag{14}$$

where $\beta = (\overline{\sigma}_t + \overline{\sigma}_c)/\overline{\sigma}_t$. Obviously, the strain rate $\dot{\varepsilon}(t)$ depends
on the load shape function $f(t)$, its derivative $df(t)/dt$ and
the relative crack opening level $CF = K_{op}/K_{max}$ (and on the yield
parameter β). At first sight it is surprising that $\dot{\varepsilon}(t)$ depends
on $1-CF = (K_{max} - K_{op})/K_{max}$ and not on the magnitude of
$K_{max} - K_{op}$. However, this is a straightforward result of
application of the definition of strain rate
$\dot{\varepsilon}(t) = d\delta(t)/\delta(t) dt$. The important role of the closure
coefficient CF in equation 14 explains why in the past some
processes were thought to be driven by crack opening, but, on
the basis of equation 14 can be governed also by the strain
rate $\dot{\varepsilon}(t)$.

Threshold and frequency effects in corrosion fatigue
     In corrosion fatigue the role of the strain rate can be
elucidated by considering the competition between strain rate
and the velocity of build-up of a passivating film shielding
the base metallic material at the crack tip from direct contact
with the environment.
If such a process is taking place then, only strain rates
larger than the overall build-up rate will allow direct contact
(and attack) of the environment on the base metal of the alloy
under consideration. This condition can be used to formulate a
criterion for initiation of accelerated fatigue crack growth.
It is assumed that, for a specific material/environment system,
crack growth acceleration initiates when a certain threshold

strain rate $\dot{\varepsilon}_{th}$ is exceeded, that is when

$$d\delta(t)/\delta(t)dt \geq \dot{\varepsilon}_{th} \tag{15}$$

Such a criterion can be used to calculate the lower bounds t_i of the periods of time $t_i \leq t \leq t_e$ during which environmentally induced crack growth acceleration occurs.
Once accelerated fatigue crack growth has initiated the crack growth rate increases. In general, the crack growth rate becomes so high that direct contact between the environment and the base metal is self-contained. To stop it the load must be brought to a hold or decreased. This implies that the period of accelerated growth ends close to the moment t_m of application of the maximum load, that is $t_e = t_m$.
Values for t_i and t_e are used, respectively, as lower and upper bounds for integration of the time dependent part of the incremental corrosion fatigue crack growth law discussed later in this section.

Using the strain rate expression 14, equation 15 can be written as

$$2f(t)df(t)/dt - \dot{\varepsilon}_{th}\left[\beta/(1-CF)^2 + f^2(t) - 1\right] \geq 0 \tag{16}$$

This equation also provides a criterion for the absence of accelerated growth associated with corrosion fatigue: If no solution for t_i can be found in the interval $t_{op} < t_i < t_m$, (t_{op} is the moment the crack is opened) then corrosion fatigue is assumed to be absent, however, other processes may take place.

In the description of crack growth under corrosion fatigue conditions we assume that the crack growth increment dc can be considered as a result of addition of a time independent part dc_f and a time dependent part dc_c, that is

$$dc = dc_f + dc_c \tag{17}$$

The first part dc_f is given by equation 3. For the time dependent part dc_c the following new basic equation is adopted

$$dc_c = C_{1c}\left[\left(K(t) - K_{op}\right)^{n_1+1} - \delta K_{thc}^{P_2}\left(K(t) - K_{op}\right)^{n_1+1-P_2} f^{P_2}(t)\right] f^{-m}(t)dt \tag{18}$$

In this equation n_1 is the same as in equation 3 and the load shape function $f(t)$ is the same as used in equations 11, 14 and 16. The shape of equation (18) is primarily chosen to be such that, after integration (see eq. 20) and superposition to the fatigue crack growth increment $\Delta c_f/\Delta N$, the simple equations 21 and 22 are obtained. This implies that C_{1c} has the same dimensions as C_1, C_2 and C in the expressions related to dc_f. In principle the threshold parameter δK_{thc} can have a value different from δK_{th} and, using similar arguments as in the

discussion of equation 5, the value of the power p_2 can be
different from p_1. Further, the reason for introduction of the
power m on the load shape function will be clarified next.
Using the load shape function, equation 11, and, after
substitution of $n_1 + 1$ by n, equation 18 can be rewritten as

$$dc_c = C_{1c}\left[(K_{max} - K_{op})^n - \delta K_{thc}^{p_2}(K_{max} - K_{op})^{n-p_2}\right]f^{n-m}(t)\,dt \qquad (19)$$

Clearly, for the case m = n the time dependent part dc_c varies
in proportion with dt. Other values of m can be used to
describe non-linear dc_c versus dt behaviour related to the load
shape function f(t). In the remaining part of this paper, it
will be assumed that, m = n.

To obtain the total crack growth increment $\Delta c/\Delta N$ for one
load cycle equation 17 must be integrated, that is

$$\Delta c / \Delta N = \Delta c_f / \Delta N + \int_{t_i}^{t_m} dc_c \qquad (20)$$

After substitution of equations 7 and 19, rearrangement of some
of the parameters and assuming that m = n, there results

$$\Delta c/\Delta N = C(K_{max} - K_{op})^n\left[1 - \left(\frac{\delta K_{th}}{K_{max} - K_{op}}\right)^{p_1} + C_c\left[1 - \left(\frac{\delta K_{thc}}{K_{max} - K_{op}}\right)^{p_2}\right](t_m - t_i)\right] \qquad (21)$$

For the specific case that $p_2 = p_1 = p$, and, $\delta K_{thc} = \delta K_{th}$
(threshold effects are assumed to be the same as in time
independent growth), equation 21 degenerates into

$$\Delta c/\Delta N = C(K_{max} - K_{op})^n\left[1 - \left(\frac{\delta K_{th}}{K_{max} - K_{op}}\right)^p\right]\left[1 + C_c(t_m - t_i)\right] \qquad (22)$$

Equation 22 demonstrates that the time dependent part acts as a
multiplier on the time independent part. On a log-log scale
this implies a shift of the crack growth curve that depends on
the frequency. Equations 21 and 22 are surprisingly simple. The
new parameters involved are: the threshold strain rate $\dot{\varepsilon}_{th}$ for
determination of t_i and, further, δK_{thc}, p_2 and C_c.
The threshold strain rate $\dot{\varepsilon}_{th}$ can be determined in a low
frequency crack growth test from the c and K versus time plots
(see Fig. 3). A value for C_c follows from the slope of the c
versus time plot obtained in the same test. Such tests are
executed at frequencies of the order 0.001 Hz. In general, the
time independent parts of equations 21 and 22 can be safely
ignored compared to the time dependent parts at such low
frequencies and the material/environment systems of interest.

As an example figure 3 is used to determine the parameters involved in the time dependent part of the crack growth law (eq. 22) and the threshold value of the strain rate $\dot{\varepsilon}_{th}$. In table 1 the quantities are listed together with the result obtained for $\dot{\varepsilon}_{th}$.
In figure 4 the measured crack growth rate is plotted versus the frequency for the same $\Delta K = 53$ MPa$\sqrt{m}$ used for the determination of the results in figure 3. Then, the value of C_c can be determined from the $\Delta c/\Delta N$ ratio measured for a high and a low frequency. After application of equation 22 for both frequencies the following equation is obtained

$$C_c = \left[\frac{(\Delta c / \Delta N)^{F=.001}}{(\Delta c / \Delta N)^{F=10}} - 1 \right] / \left(t_m^{F=.001} - t_i^{F=.001} \right) \qquad (23)$$

as $t_m^{F=10} - t_i^{F=10} = 0$. Then, it follows, that $C_c = 0.827$/sec and using this result we can predict the frequency effect shown in figure 4. The results are listed in table 2.
It is interesting to see that, for a frequency $F = .0001$ Hz, no solution for equation 16 is found. This implies that the crack growth acceleration effects diminish for frequencies lower than, say, .001 Hz. The results presented in table 2 are also plotted in figure 4.

A second example is taken from Barsom [12]. The results are reproduced in figure 5. Loading is sine shaped and the load ratio R = 0.25. Unfortunately, registrations of c versus time are not available. Therefore $\dot{\varepsilon}_{th}$ and C_c cannot be determined in the way described earlier. Some additional assumptions are to be made. Firstly, the data points obtained at a frequency F = 10 Hz are adopted as the high frequency fatigue crack growth results. Further, a closure coefficient is assumed to be CF = 0.5 and, in addition, it is assumed that $t_i = t_{op}$ for the F = 1 Hz data points, then we can determine C_c from the ratio of the crack growth rates of both data sets in the following way

$$\frac{(\Delta c / \Delta N)^{F=1Hz}}{(\Delta c / \Delta N)^{F=10Hz}} = 1 + C_c\left(t_m - t_i\right) \qquad (24)$$

It then follows $C_c = 1.2$/sec. For loading at F = 0.1 Hz the strain rates are lower and therefore $t_i > t_{op}$. From a comparison of the crack growth rates obtained for F = 0.1 Hz and F = 10 Hz, it follows that

$$\frac{(\Delta c / \Delta N)^{F=0.1Hz}}{(\Delta c / \Delta N)^{F=10Hz}} = 1 + C_c\left(t_m - t_i\right) \qquad (25)$$

From the results it is concluded that $t_i = 3.75$ sec. for the

F = 0.1 Hz series.
As threshold effects are absent we can use equation 22 to
describe the results in figure 5. The result is the same as the
dashed lines for the three frequencies indicated.
Barsom [12] also studied the effect of load wave shape on the
crack growth rate. The wave shapes used are given in figure 6.
The results are given in figure 7. From the application of the
corrosion fatigue model to the shapes of figure 6 it is
concluded that shapes 3, 4^b and 5^a and 5^b have the same common
property $t_m - t_i = 0$. Hence, the predicted crack growth rates
are the same as the high frequency fatigue data measured for
the same load amplitude and ratio R = 0.25. This is confirmed
by the measured data points in figure 7.
The load wave types 2 and 4^a in figure 6 also have a common
$t_m - t_i$ value and for the sinusoidal load the threshold strain
rate will be exceeded slightly earlier in the cycle, so, $t_i^1 <$
t_i^2 and t_i^{4a} and the crack growth rate for shape 1 will be
slightly higher than for cases 2 and 4^a. These observations are
also confirmed by the results presented in figure 7.

Implementation and verification of models
        The fatigue crack growth model has been implemented in the
NASA/FLAGRO and the ESACRACK software. The crack opening levels
K_{op} are calculated using a discretized STRIP-YIELD model. This
model has also been included in the software. An extensive
verification programme (some 500 cases) was executed to
demonstrate the accuracy and reliability of the software and
models.
The time dependent part of the model discussed in this paper
was formulated recently and is still subject of further
improvement. A verification programme is not yet formulated.

Discussion and concluding remarks
        An incremental form of crack growth law (eq. 3) was used
to derive a fatigue crack growth equation for computation of
the fatigue crack growth rate per load cycle (eq. 7).
Using the STRIP-YIELD model a criterion for initiation of
accelerated fatigue crack growth (corrosion fatigue) in a
specific environment was based on the threshold strain rate $\dot{\varepsilon}_{th}$
concept (eq. 16). A time dependent incremental growth law (eq.
18) was used to describe accelerated growth after initiation.
Using the moment in time initiation occurs as the lower bound
and the moment the load reaches its maximum level as the upper
bound, the time dependent part is integrated to obtain the
contribution per load cycle (eq. 21). In its most simple form
(eq. 22) only two new material/environment dependent parameters
are involved: the threshold strain rate $\dot{\varepsilon}_{th}$ and the parameter
C_c.
In more general situations when the low frequencies threshold
behaviour is different compared to the high frequency behaviour
two additional parameters are introduced: the threshold stress
intensity factor δK_{thc} and the threshold power p_2.
It was shown that using the most simple formulation described,
frequency and load wave shape effects can be described for some

specific environment/metal combinations.
However, it is well known that highly complicated electro-chemical, diffusion and transportation processes are taking place near the crack tip and along the crack surfaces. Clearly, the values of the parameters involved in the time dependent part of the crack growth equation highly depend on these processes and in a description of the effects of variations in the environment, such as, the electrical potential, concentration of ions, temperature and pressure, these phenomena are to be described in detail.
For the time being the equations discussed in this paper are to be considered as a specific reference solution that can be used for a description of frequency and load wave shape effects on the fatigue crack growth behaviour.

References
[1]   Elber, W., Fatigue Crack Closure under Cyclic Tension. Eng. Frac. Mech., Vol. 2, no. 1, July 1970, p.37.
[2]   Koning, A.U. de, and Dougherty, D.J., Prediction of low and high crack growth rates under constant and variable amplitude loading. Proc. of the spring meeting on "Fatigue crack growth under variable amplitude loading", (Ed. by J. Petit), Paris, 1988.
[3]   Dougherty, D.J., Koning, A.U. de, and Hillberry, B.H., Modelling high crack growth rates under variable amplitude loading, Advances in Fatigue Lifetime Predictive techniques, ASTM STP 1122, 1992, pp. 214-223.
[4]   Koning, A.U. de, Prediction of fatigue crack growth, The assessment of cracked components by Fracture Mechanics, EGF4 (Ed. by L.H. Larsen), 1989, p.61.
[5]   Koning, A.U. de, Hoeve, H.J. ten, and Henriksen, T.K., Recent advances in the modelling of crack growth under fatigue loading conditions, Proc. of the FAA/NASA Int. Symp. "Advanced Structural Integrity Methods for Airframe durability and Damage Tolerance, May 4-6, 1994, Hampton, USA.
[6]   Newman, J.C. Jr., A crack closure model for predicting fatigue crack growth under aircraft spectrum loading, ASTM STP 748, 1981, pp. 53-84.
[7]   Koning, A.U. de, and Liefting, G., Analysis of crack opening behaviour by application of a discretised STRIP-YIELD model, ASTM STP 982, 1988, pp. 437-458.
[8]   Newman, J.C., FASTRAN-II- A fatigue crack growth structural analysis program, NASA TM 104159, Febr. 1992.
[9]   Koning, A.U. de, The application of the STRIP-YIELD model in the prediction of fatigue crack growth. Final report ESA contract no. 9691-CCN4, NLR CR 97XXX L, 1997.
[10]   Speidel, M.O., Corrosion fatigue in Fe-Ni-Cr Alloys. NACE 5, Unieux-Firminy, France, June 12-16, 1973.
[11]   Döker, H., Fatigue Crack Growth Threshold: Implications, Determination and Data Evaluation. To appear in International Journal of Fatigue.
[12]   Barsom, J.H., Effect of cyclic stress form on corrosion fatigue crack propagation below K_{ISCC} in a high yield

strength steel. Corrosion Fatigue: chemistry, mechanics
and micro structure. (Eds. O. Devereux, A.J. McEvily, and
R.W. Staehle), NACE 2, June 14-18, 1971, p. 432.
Table 1--Results derived from figure 3 (R = 0.0, CF = 0.5).

time at initiation	t_i	= 367 sec.
frequency	F	= 0.001 Hz
time at end of acc. growth	t_m	= 500 sec.
value load shape function		
at initiation of acc. growth	$f(t_i)$	= 0.671
derivative of f(t)	$df(t_i)/dt$	= 0.00466/sec
threshold strain rate (eq. 16)	$\dot{\varepsilon}_{th}$	= 0.00084/sec

Table 2--The effect of frequency on the crack growth

acceleration as described by the proposed model.

frequency F Hz	t_i sec.	t_m sec.	$\Delta c/\Delta N .10^5$ m/cycle
10	0.025	0.05	1.02
1	0.25	0.5	1.21
0.1	2.5	5.0	3.07
0.01	25.7	50.0	21.1
0.001	367	500	111.0
0.0001		no initiation	

Note that the results measured for 10 Hz and 0.001 Hz were used

to determine the material parameter values C_c and $\dot{\varepsilon}_{th}$.
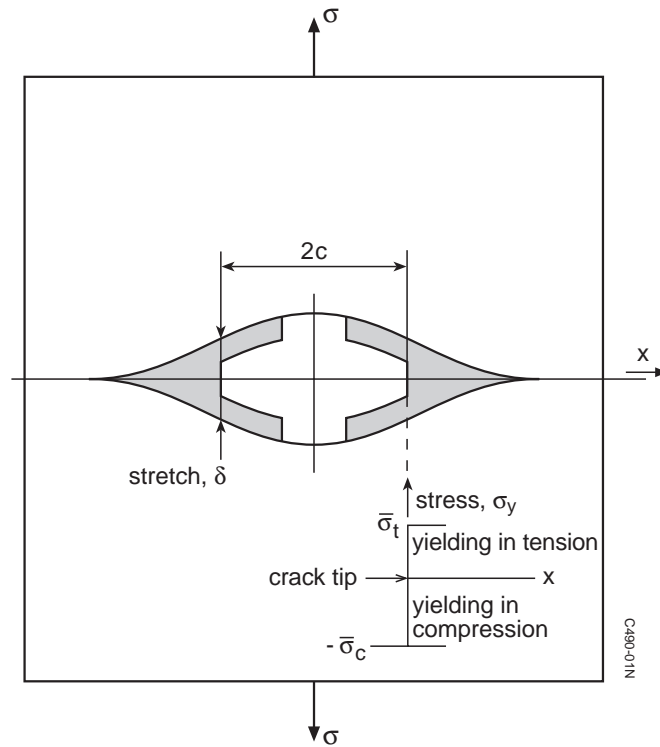
Fig. 1   The STRIP-YIELD model with different yield
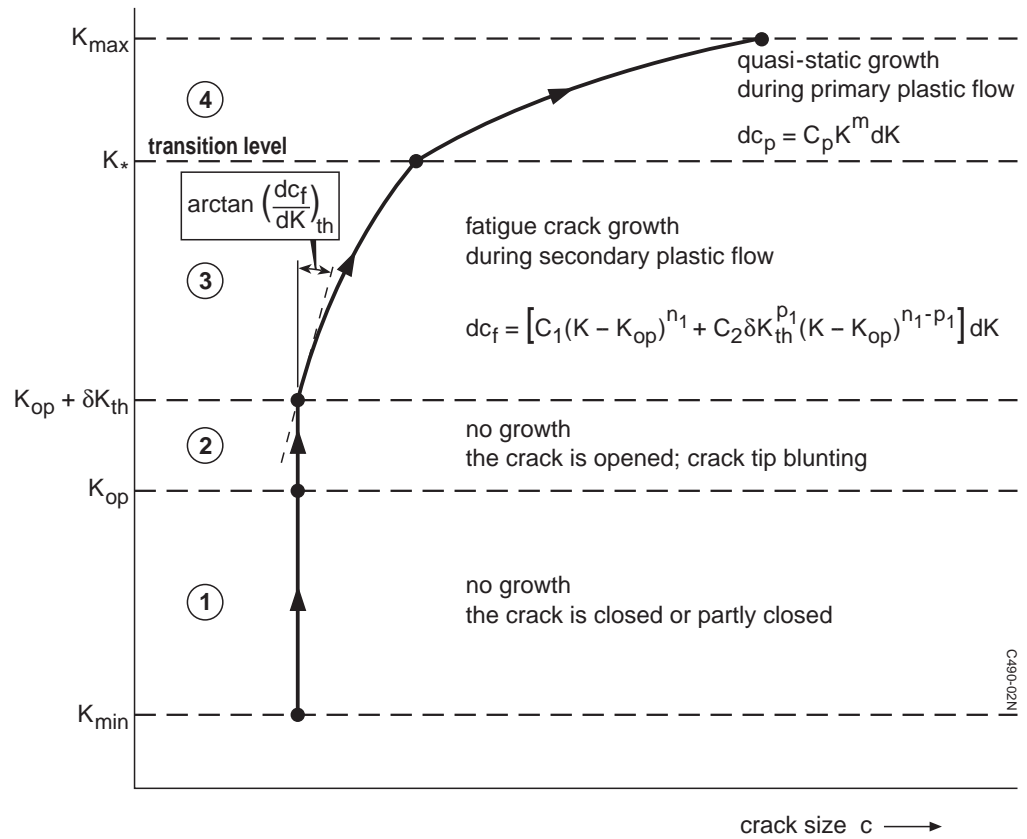limits in tension and in compression

Fig. 2   Different loading and crack growth regimes in one (half) load cycle
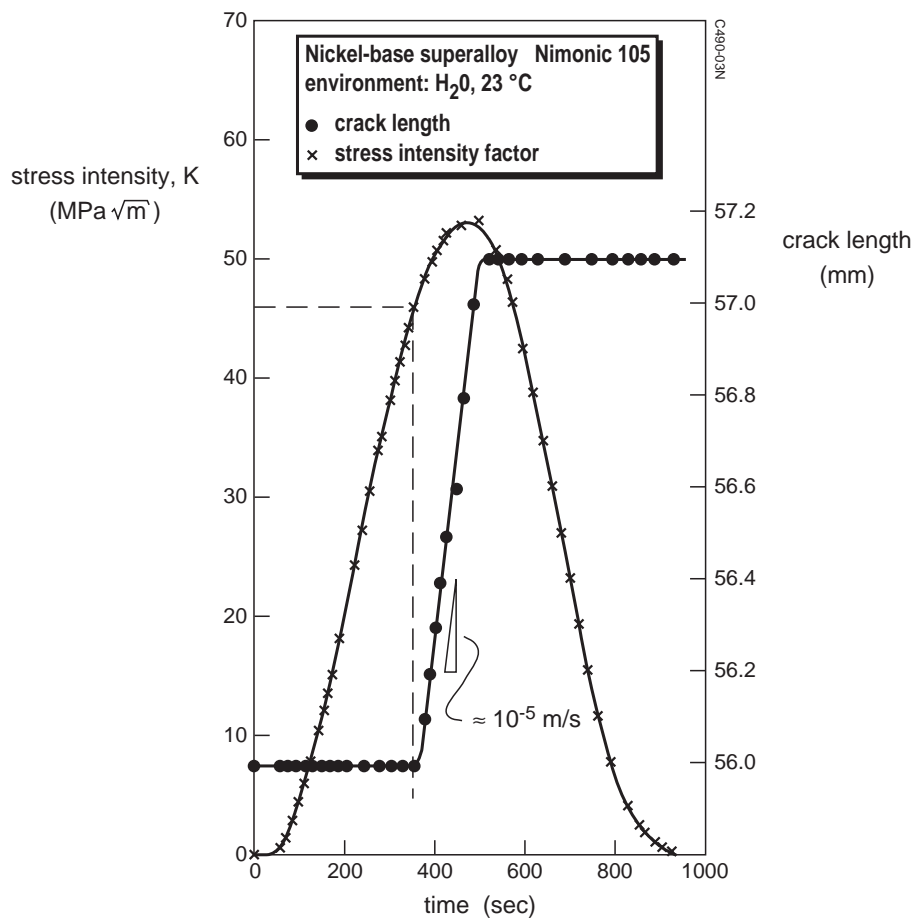
Fig. 3 A corrosion fatigue crack growing during the opening part of a load
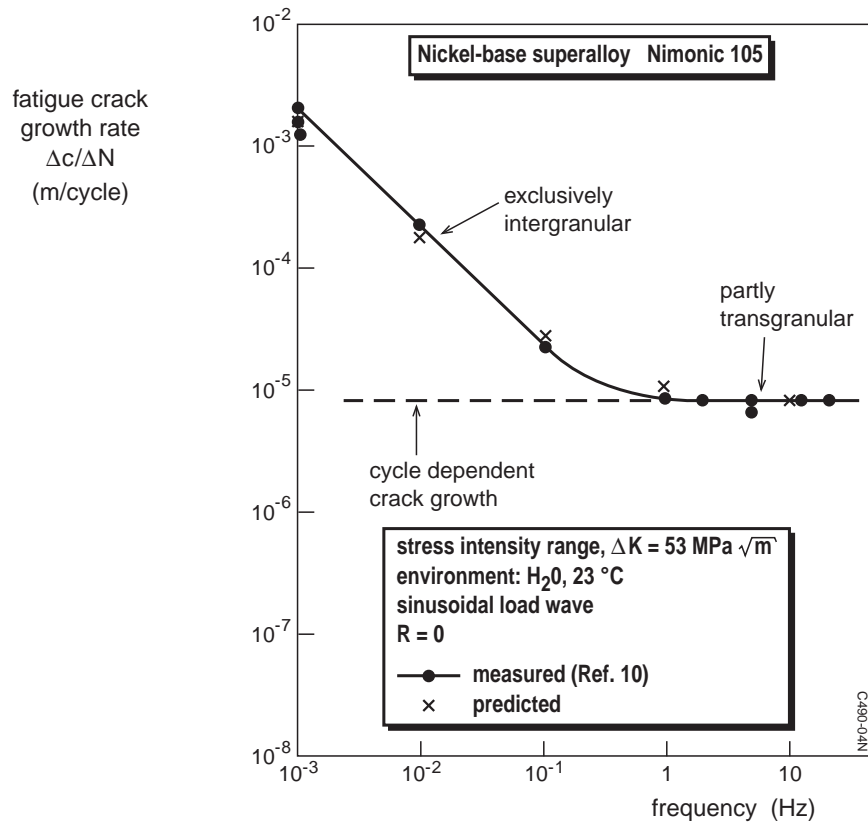cycle [10]

Fig. 4 Comparison of experimental results presented by Speidel [10]
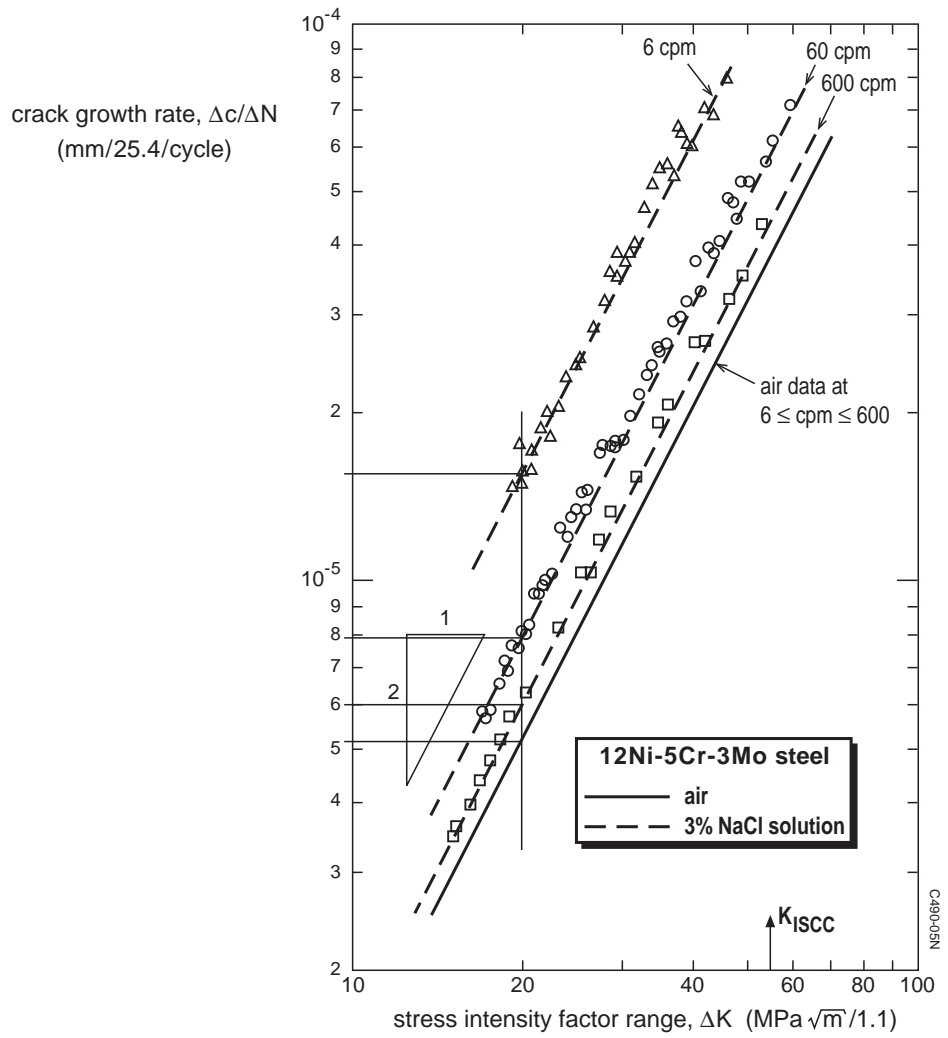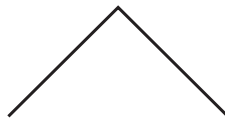and the behaviour described by the proposed model

Fig. 5 Corrosion fatigue crack growth data as a function of test frequency [12]
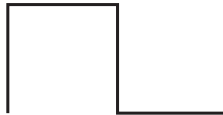
C490-06N

1   sinusoidal load

time ⟶

4   sawtooth load
4a positive   4b negative

2   triangular load

5   skewed-square load
5a reduced   5b reduced
**   min.   max.**
**   load   load**

3   square load

Fig. 6   *Various forms of cyclic stress fluctuations used for steel investigated in Ref. 12*
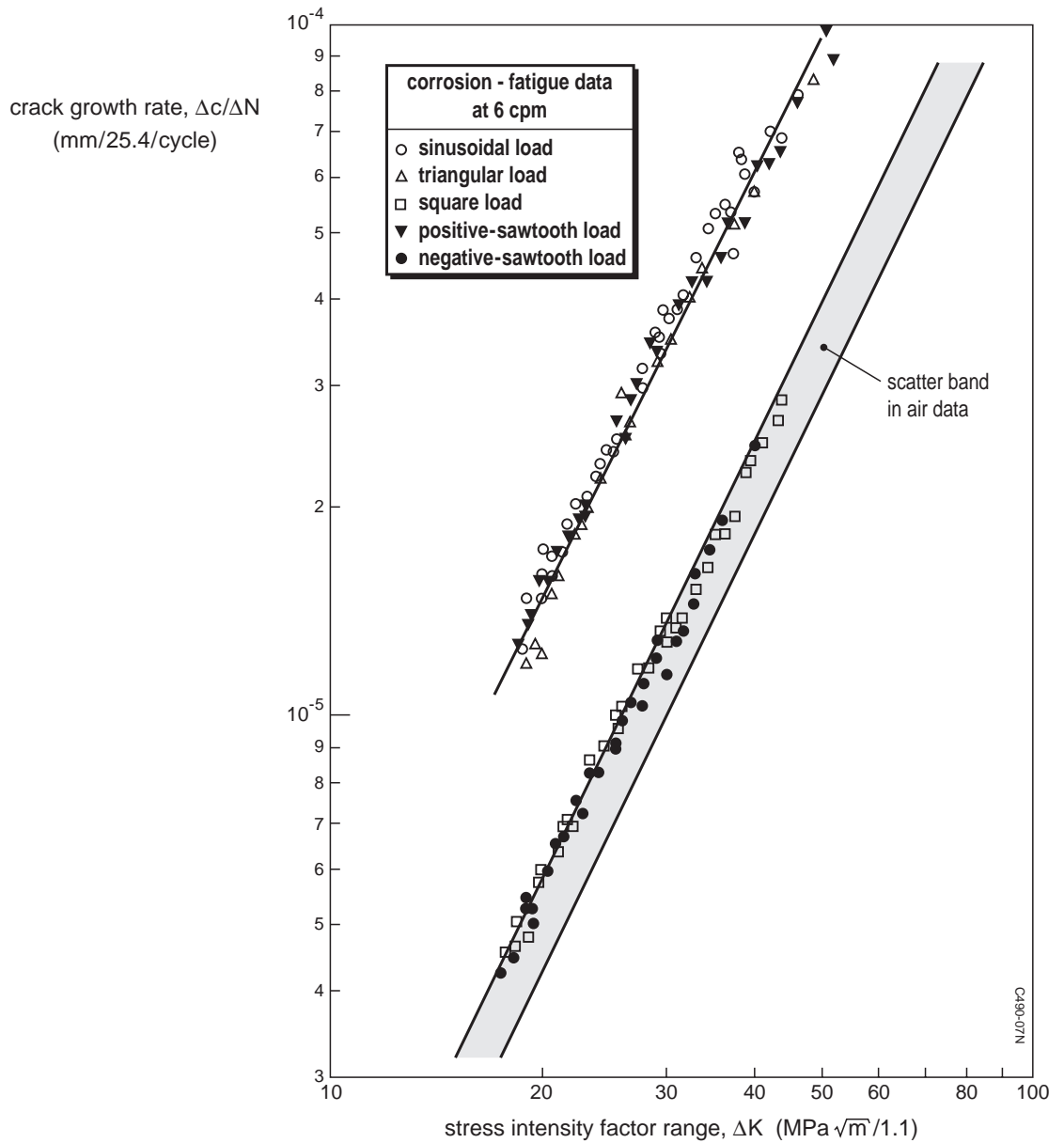
Fig. 7 *Corrosion fatigue crack growth rates in 12Ni-5Cr-3Mo steel in 3% solution of sodium chloride under various cyclic stress fluctuations with different stress - time profiles [12]*

Appendix--Load shape functions

<u>Positive saw tooth loading</u> (linear)

$$f(t) = \frac{R - CF + (1-R)t/t_m}{1 - CF}$$

<u>Sinusoidal loading</u>

$$f(t) = \frac{1 + R - 2CF + (1-R)\sin\left(\frac{\pi t}{t_m} - \frac{\pi}{2}\right)}{2(1 - CF)}$$

where $R = \dfrac{K_{min}}{K_{max}}$ and $CF = \dfrac{K_{op}}{K_{max}}$